Supporting information

Probing the Crystal and Electronic Structures of Molybdenum Oxide in Redox Process: Implications for Energy Applications

Huayu Peng,[1] Weiwei Meng,[1] He Zheng, *,[1] Yanjie Wei,[1] Huaping Sheng,[1] Huihui Liu,[1] Lei Li,[1] Guangyu Wen,[1] Shuangfeng Jia,[1] Luying Li,[2] and Jianbo Wang*,[1]

[1]School of Physics and Technology, Center for Electron Microscopy, MOE Key Laboratory of Artificial Micro- and Nano-structures, and Institute for Advanced Studies, Wuhan University, Wuhan 430072, China

[2]Center for Nanoscale Characterization & Devices, Wuhan National Laboratory for Optoelectronics, Huazhong University of Science and Technology, Wuhan 430074, China

Corresponding author email: wang@whu.edu.cn; zhenghe@whu.edu.cn.

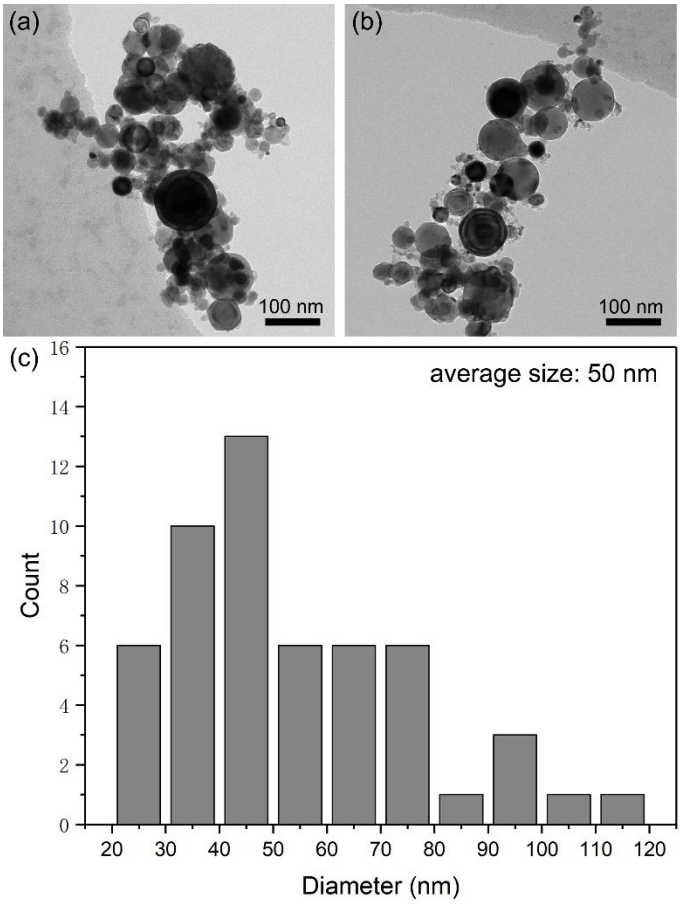

Figure S1. (a, b) The BF images of Mo NPs and (c) their size distributions.

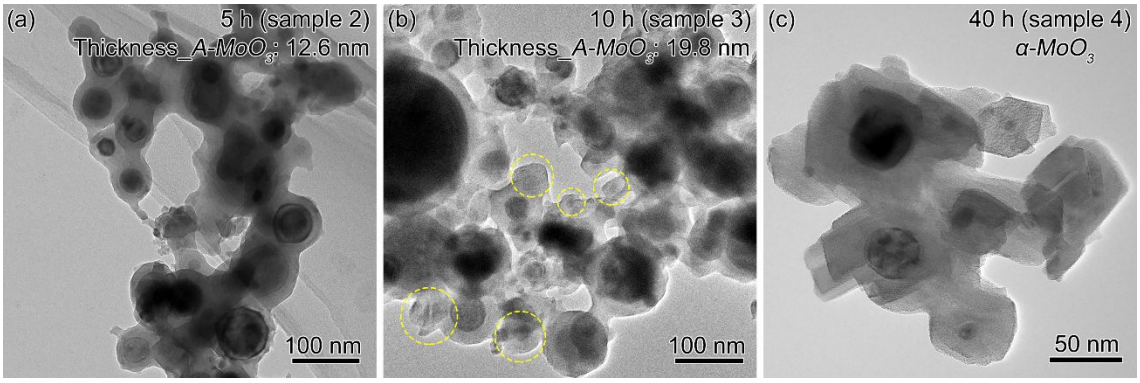

Figure S2. (a) The BF image of sample 2 and the average thickness of A-MoO_3 shell is 12.6 nm. (b) The BF image of sample 3 and the average thickness of A-MoO_3 shell is 19.8 nm (yellow

circles represent the oxide layers are crystalline). (c) The BF image of sample 4, whose oxide layers are α-MoO_3 nanosheets.

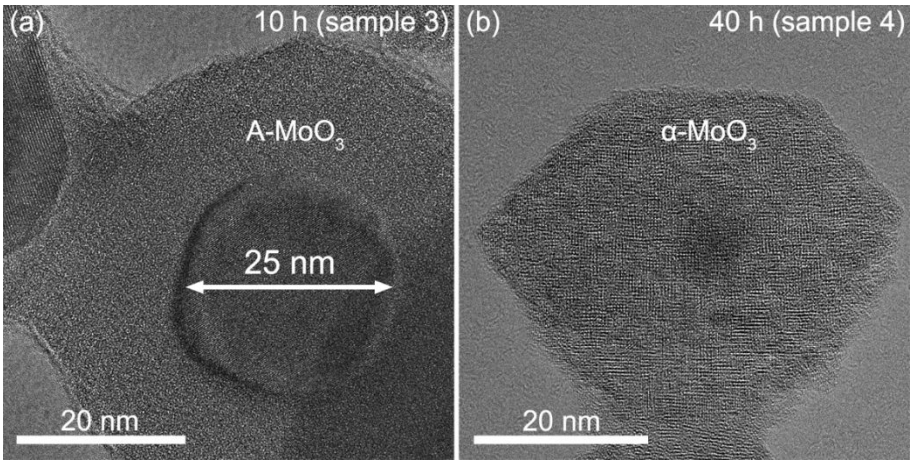

Figure S3. The nucleation of A-MoO_3 (a) followed by the nucleation of α-MoO_3 (b) after 10 h and 40 h heat treatment in the Mo NP with a diameter of approximately 25 nm.

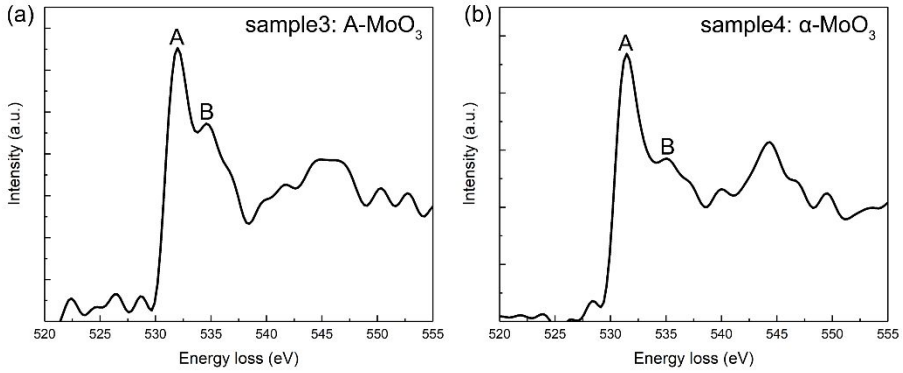

Figure S4. The EELS spectra recorded on the amorphous and crystalline oxide layers of samples 3 (a) and 4 (b), respectively.

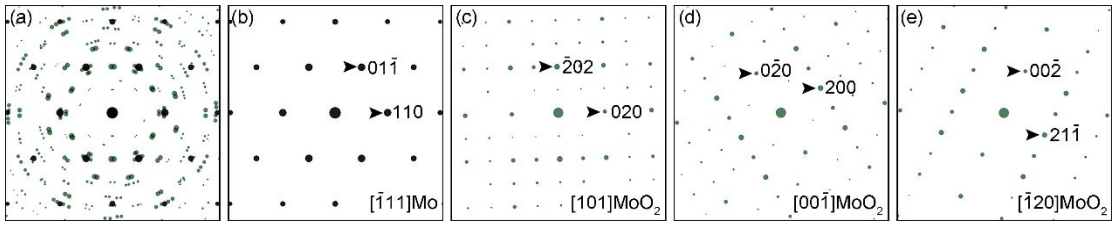

Figure S5. (a) The composite simulated SAED pattern of the NP with the coexistence of Mo: (b) $[\bar{1}11]_{Mo}$, and three types of MoO_2: (c) $[101]_{MoO_2}$, $[\bar{1}0\bar{1}]_{MoO_2}$, (d) $[00\bar{1}]_{MoO_2}$, $[001]_{MoO_2}$, (e) $[\bar{1}20]_{MoO_2}$ and $[1\bar{2}0]_{MoO_2}$ variants.

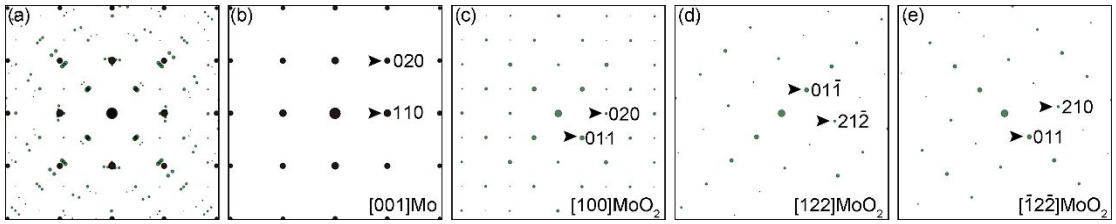

Figure S6. (a) The composite simulated SAED pattern of the NP with the coexistence of Mo: (b) $[001]_{Mo}$, three types of MoO_2 (c) $[100]_{MoO_2}$, $[\bar{1}00]_{MoO_2}$, (d) $[122]_{MoO_2}$, $[\overline{122}]_{MoO_2}$, (e) $[\bar{1}2\bar{2}]_{MoO_2}$ and $[1\bar{2}2]_{MoO_2}$ variants.

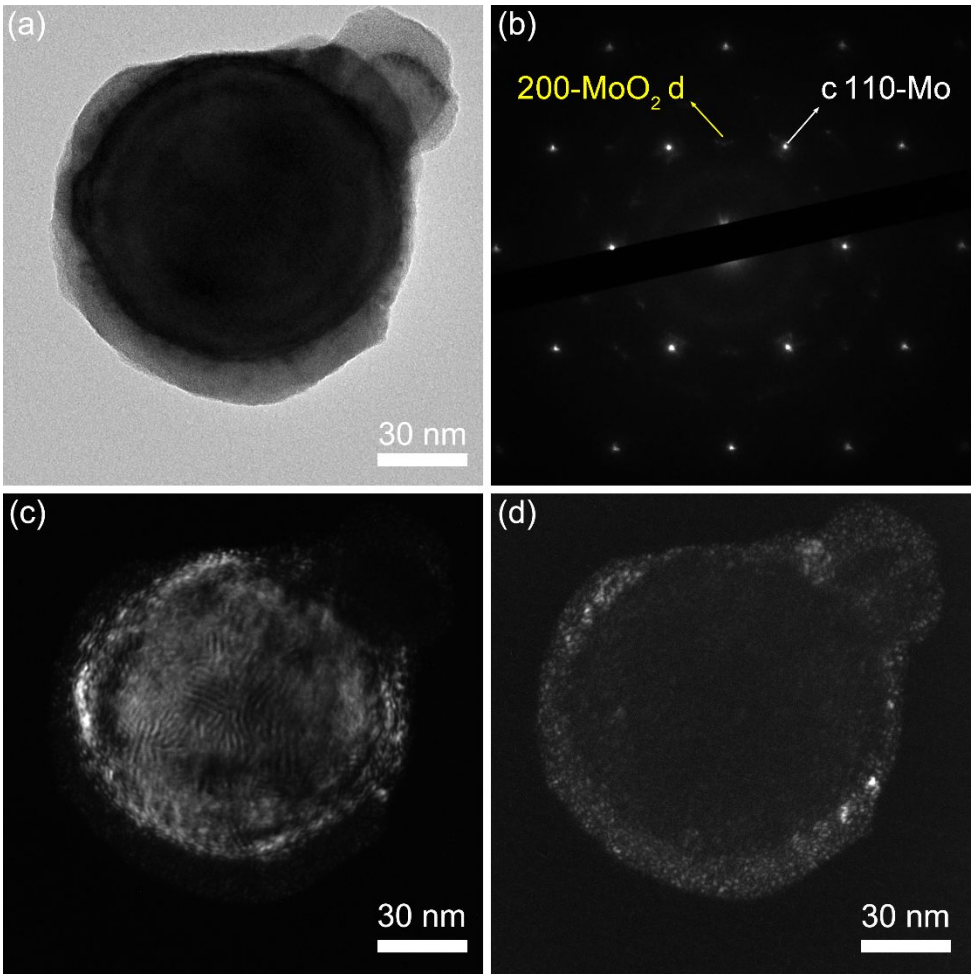

Figure S7. (a) The BF image and the corresponding SAED pattern (b) of a core-shell NP after e-beam irradiation. (c) DF images acquired by sequentially selecting $(110)_{Mo}$ and $(200)_{MoO_2}$ diffraction spots from the diffraction pattern in (b).

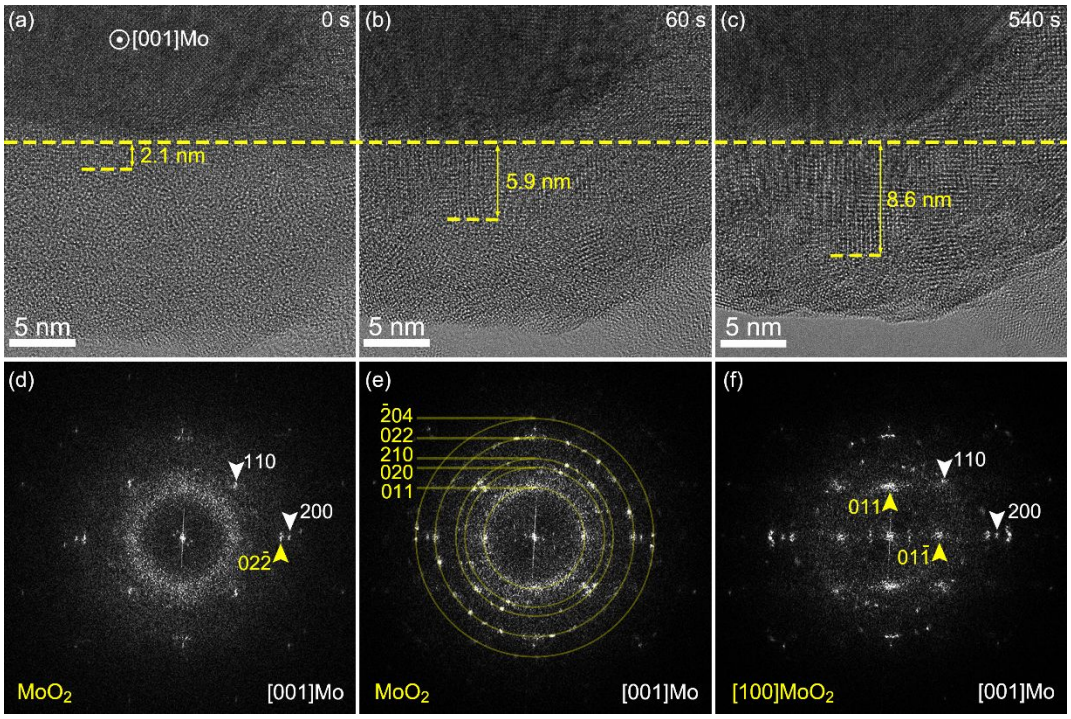

Figure S8. (a-c) *In-situ* HRTEM images of a single Mo/A-MoO_3 core-shell NP under e-beam irradiation. (d-f) The FFT images corresponding to (a-c) respectively.

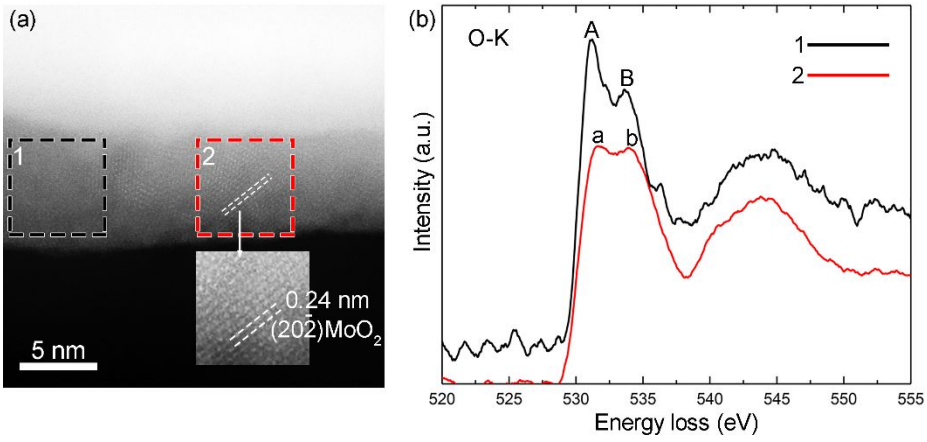

Figure S9. (a) HAADF-STEM image of a Mo/A-MoO_3 core-shell NP. (b) EELS spectra recorded on unirradiated and irradiated A-MoO_3 shell in (a) showing the ELNES of O-K edges.

E-beam effect during the reduction

There are several mechanisms for the interactions between e-beam and materials in TEM/STEM, including elastic (knock-on effects) and nonelastic collisions (radiolysis, thermal effects) between electrons and atoms.[1] Generally, the irradiation effects of conductor materials are dominated by elastic scattering, while non-conductor materials are mainly affected by inelastic scattering. Based on the knock-on mechanism, the maximum kinetic energy acquired by the O atom at 200 kV is 32.8 eV. There is no report on the threshold displacement energy of the O atom in A-MoO_3, while in most oxides the value is more than 40 eV.[1] Furthermore, the surface threshold displacement energy should be one-fifth of the bulk displacement energy in most cases.[1] Therefore, the knock-on effect is more likely to cause sputtering of the surface O atom in A-MoO_3 layer mainly in the surface area. However, the *in-situ* HRTEM observation indicates that the reduction of A-MoO_3 initially occurred closed to the metal core (Figure S8), indicating that the knock-on effect may not be the main cause.

The theoretical calculations indicate that α-MoO_3 with 1.95 eV indirect bandgap is a semiconductor, while MoO_2 is metallic (Figure 7).[2] Therefore, the inelastic scattering effect should be considered: (1) Thermal effects. Figure S10a shows a single NP whereas a small portion of the NP was irradiated. It is noticed that the crystallization only occurred within the area irradiated by the e-beam (Figure S10b), illustrating that the heating effect does not play a major role;[1] (2) radiolysis. Since Mo^{6+} has no valence electrons, when the core electrons of A-MoO_3 shell are

ionized by the incident electrons, the valence electrons of O^{2-} fill into the holes, and the energy released by this process can cause another valence electron of O^{2-} to be emitted in Auger electron. In this sense, O^0 and even O^+ are produced, resulting in the desorption of O atom[1] and the reduction of A-MoO_3 to monoclinic MoO_2. After the formation of conductive MoO_2, the radiolysis effect is negligible which explains why the MoO_2 structures were pretty stable (Figure 4e) and did not further reduce into Mo metals under irradiation. Moreover, the rate of crystallization is beam current density dependent. It takes ~10 min to form MoO_2 at an electron beam current density of ~1 A/cm^2, and only ~1 min at ~10^3 A/cm^2, which is in accordance with the characteristics of radiolysis mechanism. As such, the radiolysis plays a major role in the crystallization of A-MoO_3 rather than knock-on effects.

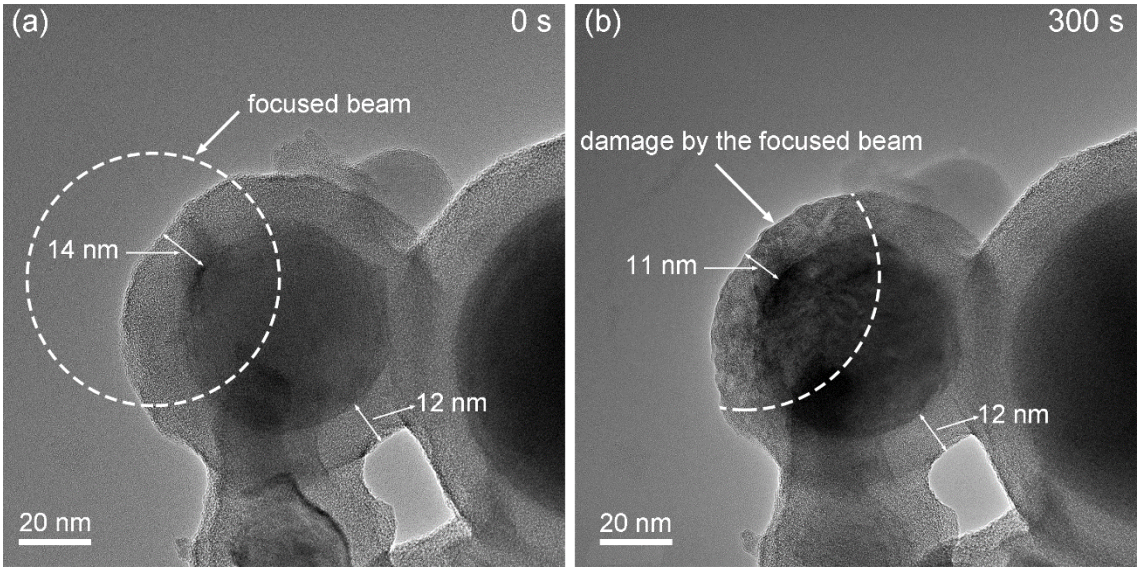

Figure S10. (a, b) Low-magnification TEM image showing the Mo/A-MoO_3 core-shell NP before (a) and after 300 s e-beam irradiation (b). The white dotted circle indicates the area irradiated by the e-beam.

References

(1) Jiang, N., Electron beam damage in oxides: A review. *Rep. Prog. Phys.* **2016,** *79*, 016501.
(2) Scanlon, D. O.; Watson, G. W.; Payne, D. J.; Atkinson, G. R.; Egdell, R. G.; Law, D. S. L., Theoretical and experimental study of the electronic structures of MoO_3 and MoO_2. *J. Phys. Chem. C* **2010,** *114*, 4636-4645.